Journal of Orthopaedic Translation 48 (2024) 133–145

Contents lists available at ScienceDirect

Journal of Orthopaedic Translation

journal homepage: www.journals.elsevier.com/journal-of-orthopaedic-translation

Original Article

Phillygenin inhibits neuroinflammation and promotes functional recovery after spinal cord injury via TLR4 inhibition of the NF-κB signaling pathway

Yu Zhang [a,b,1], Shining Xiao [b,c,1], Fan Dan [a,b], Geliang Yao [a,b], Shu'e Hong [a], Jiaming Liu [a,b], Zhili Liu [a,b,*]

[a] Department of Orthopedics, The First Affiliated Hospital, Jiangxi Medical College, Nanchang University, Nanchang, 330006, China
[b] Jiangxi Provincial Key Laboratory of Spine and Spinal Cord Diseases, Nanchang, China
[c] Department of Rehabilitation Medicine, The First Affiliated Hospital, Jiangxi Medical College, Nanchang University, Nanchang, 330006, China

ARTICLE INFO

Keywords:
Neuroinflammation
Neuronal apoptosis
NF-κB signaling pathway
Phillygenin
Spinal cord injury

ABSTRACT

Background: Spinal cord injuries (SCIs) trigger a cascade of detrimental processes, encompassing neuroinflammation and oxidative stress (OS), ultimately leading to neuronal damage. Phillygenin (PHI), isolated from forsythia, is used in a number of biomedical applications, and is known to exhibit anti-neuroinflammation activity. In this study, we investigated the role and mechanistic ability of PHI in the activation of microglia-mediated neuroinflammation and subsequent neuronal apoptosis following SCI.

Methods: A rat model of SCI was used to investigate the impact of PHI on inflammation, axonal regeneration, neuronal apoptosis, and the restoration of motor function. *In vitro*, neuroinflammation models were induced by stimulating microglia with lipopolysaccharide (LPS); then, we investigated the influence of PHI on pro-inflammatory mediator release in LPS-treated microglia along with the underlying mechanisms. Finally, we established a co-culture system, featuring microglia and VSC 4.1 cells, to investigate the role of PHI in the activation of microglia-mediated neuronal apoptosis.

Results: In vivo, PHI significantly inhibited the inflammatory response and neuronal apoptosis while enhancing axonal regeneration and improving motor function recovery. *In vitro,* PHI inhibited the release of inflammation-related factors from polarized BV2 cells in a dose-dependent manner. The online Swiss Target Prediction database predicted that toll-like receptor 4 (TLR4) was the target protein for PHI. In addition, Molecular Operating Environment software was used to perform molecular docking for PHI with the TLR4 protein; this resulted in a binding energy interaction of −6.7 kcal/mol. PHI inhibited microglia-mediated neuroinflammation, the production of reactive oxygen species (ROS), and activity of the NF-κb signaling pathway. PHI also increased mitochondrial membrane potential (MMP) in VSC 4.1 neuronal cells. In BV2 cells, PHI attenuated the overexpression of TLR4-induced microglial polarization and significantly suppressed the release of inflammatory cytokines.

Conclusion: PHI ameliorated SCI-induced neuroinflammation by modulating the TLR4/MYD88/NF-κB signaling pathway. PHI has the potential to be administered as a treatment for SCI and represents a novel candidate drug for addressing neuroinflammation mediated by microglial cells.

The translational potential of this article: We demonstrated that PHI is a potential drug candidate for the therapeutic management of SCI with promising developmental and translational applications.

Abbreviations: BBB, Basso Beattie Bresnahan; CETSA, Cellular thermal shift assay; CNS, Central nervous system; DMSO, Dimethyl sulfoxide; LPS, Lipopolysaccharide; MEP, Motor-evoked potential; MMP, Mitochondrial membrane potential; OS, Oxidative stress; PHI, Phillygenin; PPI, Protein interaction; qRT-PCR, quantitative real-time polymerase chain reaction; ROS, Reactive oxygen species; SCI, Spinal cord injury; SD, Sprague Dawley; TLR4, Toll-Like Receptor 4; WB, Western blot.

* Corresponding author. The First Affiliated Hospital, Jiangxi Medical College, Nanchang University, No. 17 Yongwaizheng Street, Donghu District, Nanchang, 330006, Jiangxi Province, China.
E-mail address: zhili-liu@ncu.edu.cn (Z. Liu).

[1] Yu Zhang and Shining Xiao contributed equally to this work.

https://doi.org/10.1016/j.jot.2024.07.013
Received 6 March 2024; Received in revised form 11 July 2024; Accepted 29 July 2024

1. Introduction

Spinal cord injury (SCI) is a serious neurological disorder that affects millions of individuals worldwide and causes motor, sensory, and autonomic dysfunction [1,2]. The initial traumatic injury can damage the spinal cord or cause structural damage, followed by a range of secondary injuries, including inflammation, oxidative stress (OS), apoptosis, and neuronal loss, ultimately leading to motor dysfunction [3]. Currently, the management of SCI predominantly focuses on strategies to prevent and mitigate secondary damage [4,5]. However, there is a lack of well-defined and effective therapeutic agents in current clinical practice [6–8]; consequently, there is an urgent need to investigate potential pharmacological interventions for the management of SCI.

Neuroinflammation plays a pivotal role in the secondary injuries associated with SCI [9–11] and the microglia play a pivotal and irreplaceable role in neuroinflammation within the central nervous system (CNS) [12,13]. Following SCI, the microglia are rapidly activated, thus leading to the upregulation of pro-inflammatory cytokines mediated by various signaling cascades [14]. Excessive activation of the microglia results in the release of numerous pro-inflammatory factors, including IL-1β, TNF-α, and reactive oxygen species (ROS), which further exacerbate inflammation [11]. Simultaneously activated microglial cells can also exert toxic effects on neurons, and are therefore crucial for the recovery of sensory and motor function following SCI [15]. Therefore, the key to a patient recovering from SCI is to inhibit activation of the microglia at the site of injury and to control the subsequent inflammatory response.

Over recent years, numerous monomers derived from traditional Chinese medicine have garnered significant attention for their potential to treat SCI, particularly by virtue of their low levels of toxicity and reduced side effects [16,17]. Phillygenin (PHI) [18] is the main active ingredient of forsythia, a plant that is commonly used in traditional medicine, and exhibits several important biological properties, including anti-inflammatory effects [18], the amelioration of non-alcoholic fatty liver [19], improvements in the intestinal mucosal barrier [20], and the inhibition of pancreatic cancer cell survival [21]. Moreover, PHI has shown significant potential for mitigating liver fibrosis induced by carbon tetrachloride [22]. Nevertheless, the pharmacological effects of PHI on SCI have yet to be elucidated.

In this study, we investigated the pharmacological effects of PHI on the progression of SCI. We found that PHI exerted anti-neuroinflammatory effects by inactivating the NF-κB signaling pathway by targeting TLR4. The purpose of this study was to investigate the potential neuroprotective activity of PHI on anti-neuroinflammatory effects and functional recovery during the treatment of SCI. Our findings have promising implications for the development of novel therapeutic agents based on the pathogenesis of SCI.

2. Materials and methods

2.1. Animals

A total of 60 female Sprague Dawley rats (approximately 220 g in weight and eight weeks-of-age) were sourced from Zhejiang Weitong Lihua Experimental Animal Technology Co., Ltd(Zhengjiang, China). Food and water were provided *ad libitum* to rats in a temperature-controlled environment.

2.1.1. PHI reagents and cell culture

PHI (CAS. 487-39-8, purity ≥98 %) was purchased from GlpBiotechnology Co., Ltd. (Montclair, USA). PHI was dissolved in Dimethyl sulfoxide(DMSO, MCE, USA) reagent, and lipopolysaccharide (LPS) was diluted to 1 μg/mL (Merck, Germany). The BV2 microglial cell line and the VSC4.1 spinal cord anterior horn motor neuron tumor cell line were obtained from Procell Life Science & Technology Co., Ltd. (Wuhan, China). Cells were cultured in DMEM (4.5 g/L glucose) supplemented with 10 % FBS in a humidified incubator at 37 °C with 5 % carbon dioxide.

2.2. SCI model and treatment

All rats were randomly assigned to one of three groups, each containing 20 rats: a Sham operation group, a SCI group, and avSCI + PHI group. Under sterile conditions, all rats were anesthetized via an intraperitoneal injection of 1 % sodium pentobarbital (50 mg/kg). Then, we induced SCI by exposing the spinal cord at the T9–T10 level and applying a vascular clip to the spinal cord tissue for 3 s to induce crush damage. Rats in the treatment group were given an intraperitoneal injection of PHI (50 mg/kg) immediately after the occurrence of SCI, with continued administration for 7 days.

2.3. Functional behavior evaluation

Hindlimb movement recovery was assessed by the Basso Beattie Bresnahan (BBB) motor rating scale on days 0, 1, 3, 7, 14, 21, 28, 35, and 42 post-surgery. On day 21 and until day 42 post-surgery, the rats in each group were subjected to footprint analysis and electrophysiological (MEP) evaluation. Behavioral experiments were scored by authors who were blinded to the experimental conditions.

2.4. Histology

On day 42 post-surgery, spinal cord tissues, along with other major organ tissues, including the heart, spleen, liver, kidney, and lungs, were collected from rats in each group. These tissues were fixed in 4 % paraformaldehyde, dehydrated, paraffin embedded, and subsequently sectioned for hematoxylin and eosin staining.

2.5. Immunofluorescent staining of cells and sections

For *in vitro* experiments, BV2 and VSC4.1 cells were seeded onto 20 mm diameter glass slides placed within six-well plates. After rinsing with PBS, we applied 0.5 % Triton X-100 to disrupt cell membranes, followed by 5 % bovine serum albumin (BSA) to block the cells. Tissue sections were dewaxed in xylene and dehydrated with a series of graded ethanol concentrations. Following EDTA antigen–antibody repair, the sections were blocked with 5 % BSA. Cell cultures and spinal cord tissues were subsequently incubated overnight at 4 °C with appropriate primary antibodies. The following morning, the sections were washed in PBS and then incubated with appropriate fluorescent secondary antibodies for 1 h at room temperature. After additional washing steps, an anti-fluorescence quencher (including DAPI) was added and the slides were covered and sealed. Representative images were captured by a confocal laser scanning microscope (Leica, Germany) and subsequently analyzed by ImageJ software(National Institutes of Health, NIH, USA). The following antibodies were employed in this study: anti-CD68 (1:400; Abcam), anti-Iba-1 (1:400; Abcam), anti-CD11b (1:400; Abcam), anti-p65 (1:400; CST), anti-GFAP (1:500; CST), anti-NeuN (1:200; CST), anti-Bcl-xL (1:400; CST), anti-GAP43 (1:200; CST), and anti-MAP2 (1:200; CST).

2.6. Cell viability assays

BV2 cells were seeded into 96-well plates and subsequently exposed to gradient concentrations of PHI (0, 12.5, 25, 50, 100, 200, or 400 μg/mL) for a 24-h incubation period. Subsequently, 10 % of the volume of culture medium was supplemented with CCK-8 reagent followed by incubation for 2 h. Finally, we used a microplate reader (Thermo, USA) to measure the absorbance at a wavelength of 450 nm, thus allowing us to calculate the optical density.

2.7. Plasmid construction and transfection

A TLR4 overexpression plasmid (PLV3-CMV-TLR4) and an empty PLV3-CMV vector were obtained from Miaoling Biology (Wuhan, China). The TLR4 plasmid was transfected into HEK 293T cells at a density of 60%–70 %. After 48 h, the lentivirus supernatant was collected, and a Lentivirus Concentration Solution (YiSheng, Shanghai, China) was used to increase the virus titer. When the fusion rate of BV2 microglia reached 30%–40 %, the virus was mixed into the culture medium for infection.

2.8. Co-culture of cells

BV2 microglial cells and neuronal VSC 4.1 cells were co-cultured using a Transwell system with 0.4 μm wells in a six-well plate. Initially, BV2 cells were pretreated with PHI (at concentrations of 0, 25, 50, or 100 μg/mL) for 24 h. Subsequently, the cells were stimulated with 1 μg/mL of LPS or left unstimulated, based on the experimental grouping. Following washing with PBS, the BV2 cells were co-cultured with VSC 4.1 cells in six-well plates. After 24 h of co-culture, immunofluorescence and western blotting (WB) were used to determine the expression of key markers.

2.9. WB analysis

Total proteins were separated by SDS-PAGE and transferred to PVDF membranes (Millipore). Next, the membranes were blocked with 5 % skimmed milk and then incubated overnight at 4 °C with the following antibodies: Iba-1 (1:2000), Bcl-xL (1:1000), CD68 (1:2000), iNOS (1:1000), GAP43 (1:1000), COX-2 (1:2000), MAP2 (1:1000), p65 (1:2000), phosphorylated (p)-p65 (1:1000), IκBα (1:1000), phosphorylated (p)-IκBα (1:1000), NeuN (1:1000), GAPDH (1:4000), and β-actin (1:5000); all antibodies were obtained from Cell Signaling Technology (Danvers, MA, USA). The following morning, membranes were washed with TBST and incubated with appropriate secondary antibodies. Finally, we used Image Lab software (Bio-Rad) to analyze the membranes and Image J to perform quantitative analysis.

2.10. qRT-PCR

Total RNA was extracted from BV2 cells with a Universal RNA Purification Kit (EZBioscience, Shanghai), followed by reverse transcription. Quantitative PCR (qPCR) was then conducted with a SYBR real-time fluorescence quantitative PCR kit (Vazyme, China). Table S1 provides a comprehensive list of all primer sequences employed in this investigation.

2.11. Live/dead staining

Following co-culture, VSC 4.1 cells were washed 1–2 times in buffer and then treated with Calcein-AM and PI. Samples were then incubated in the dark at room temperature for 15–30 min. Finally, the cells were washed three times in buffer to eliminate excess dye. Fluorescence images were then acquired with an inverted fluorescence microscope (ZEISS, Germany).

2.12. Detection of intracellular ROS

The levels of ROS in VSC4.1 cells were evaluated with a DCFH-DA probe (10 μM). In brief, cells underwent 1–2 washes with buffer washes and then incubated in the dark with DCFH-DA for approximately 30 min. Subsequently, cells were rinsed three times with buffer, and fluorescence images were captured with an inverted fluorescence microscope (ZEISS, Germany).

2.13. Bioinformatic analysis

Next, we predicted the target protein for the PHI monomer (PubChem CID: 3083590) by utilizing Swiss Target Prediction(http://www.swisstargetprediction.ch/), the SEA database(http://sea.bkslab.org/), and the HERB database(http://herb.ac.cn/). By performing comparisons with proteins related to inflammation, we considered the common proteins identified in both sets of results as potential target proteins for PHI in the context of inflammatory-related diseases. These overlapping target proteins were then used to construct signaling pathway networks. Subsequently, these networks were uploaded to the STRING database (https://string-db.org/cgi/input.pl) and Cytoscape(http://www.cytoscape.org/) to create protein–protein interaction (PPI) networks. Key proteins were subsequently identified by topology analysis and MCODE cluster analysis. PHI was then experimentally docked with the TLR4 protein (protein number: 4G8A) by AutoDock Vina software(https://vina.scripps.edu/), and the free binding energy was calculated.

2.14. Statistical analysis

Data are presented as means ± standard deviation (SD) and the Shapiro–Wilk test was used to test whether data were normally distributed. Tukey's multiple-comparison test was used in conjunction with one-way and two-way analysis of variance for significance testing. GraphPad Prism 9.0(GraphPad Software, USA) was used for all data analysis. $p < 0.05$ was considered statistically significant.

3. Results

3.1. PHI ameliorated pathology and motor function in a rat model of SCI

First, we evaluated the impact of PHI on functional recovery in rats following SCI by applying the BBB open-field locomotor test in conjunction with footprint analysis. Analysis indicated that the group treated with PHI exhibited significantly superior motor function when compared to the SCI group without PHI treatment (Fig. 1A–H; $p < 0.05$). In addition, electrophysiological analysis revealed that the magnitude of MEP potentials was higher in rats from the PHI group (Fig. 1K–M). Compared to the SCI group, histological analyses of tissue sections stained with H&E demonstrated a significant reduction in the longitudinal and transverse cavity areas of rats from the PHI group (Fig. 1I and J). These data suggest that PHI can significantly promote the regeneration of spinal cord tissue, reduce cavity volume, and enhance motor function recovery following SCI.

Next, we evaluated the biological safety of PHI. Forty-two days after SCI surgery, we harvested the internal organs of experimental rats that had been treated with and without PHI. Tissue sections were then prepared and stained with H&E for morphological examination. No significant disparities were detected between the PHI-treated group and the Sham group in terms of morphology (see Fig. S1), thus confirming that PHI treatment was not toxic to the experimental rats.

3.2. PHI suppressed microglial activation and attenuated inflammation

To comprehensively evaluate the impact of PHI on microglial activation following SCI, we next conducted immunostaining to quantify the presence of activated microglia, as indicated by Iba-1 and CD68 immunostaining in sections of spinal cord tissue. A significant reduction in the number of Iba-1- and CD68-positive microglia was detected both within and surrounding the site of SCI in the PHI-treated group when compared to the SCI group (Fig. 2A–D, Fig. S2; $p < 0.05$). Furthermore, the expression levels of inflammatory markers, including iNOS and COX-2, as well as the levels of microglia-associated proteins (Iba-1 and CD68), were significantly elevated in rats from the SCI group when compared to the Sham group; however, these changes were effectively mitigated by PHI treatment (Fig. 2E–H, Fig. S2; $p < 0.05$). Collectively,

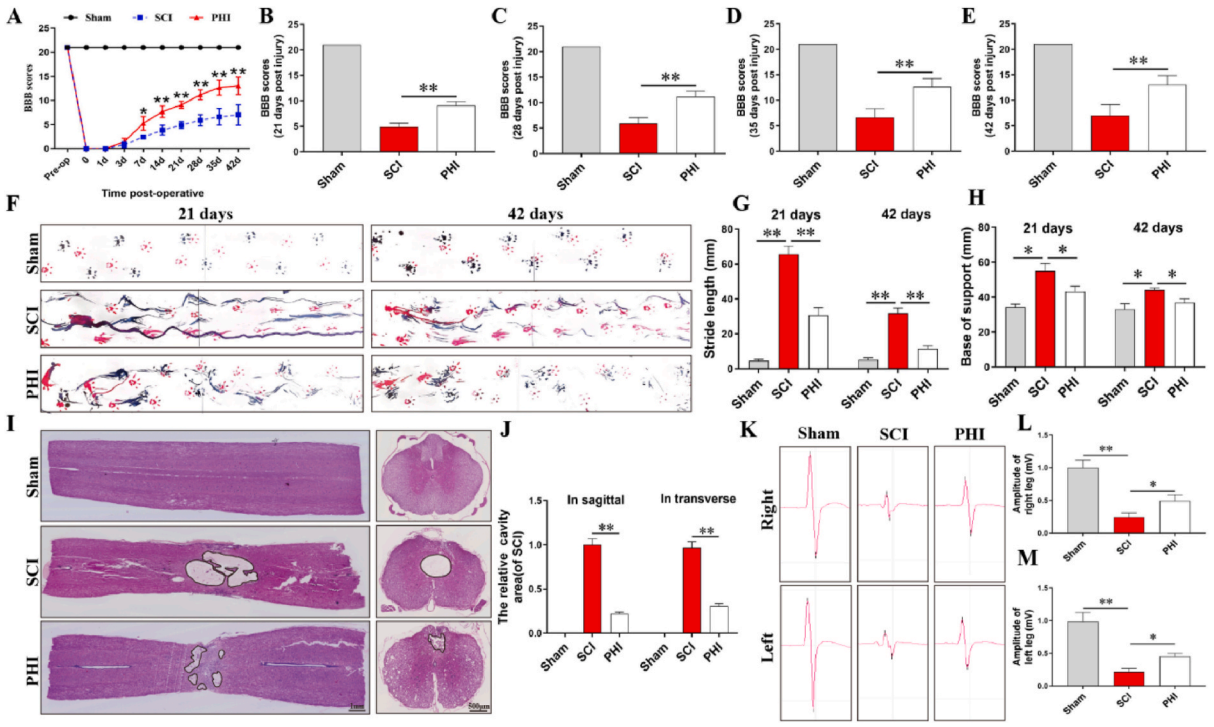

Figure 1. Phillygenin improved motor function recovery in rats following spinal cord injury (SCI). (**A**) BBB scores at different time points after SCI in three groups of rats. (**B–E**) Analysis of BBB scores at 21-, 28-, 35-, and 42-days post-injury. (**F**) Footprint analysis at 21 and 42 days post-SCI to assess hindlimb motor function recovery. (**G, H**) Quantitative assessment of footprint at 21 and 48 days post-injury to evaluate motor recovery. (**I, J**) Schematic representation and quantification of the cavity area in spinal cord tissue at 42-days post-injury. (**K**) Motor-evoked potential (MEP) amplitude results from electrophysiology experiments for the three groups of rats. (**L, M**) Quantitative bar graphs showing motor-evoked potential (MEP) amplitudes for each group. (n = 10–12 per group for BBB scores, n = 3 per group for footprint assays, electrophysiology experiments and H&E staining at 42 days post-injury). Data are presented as mean ± SD, *P < 0.05 and **P < 0.01.

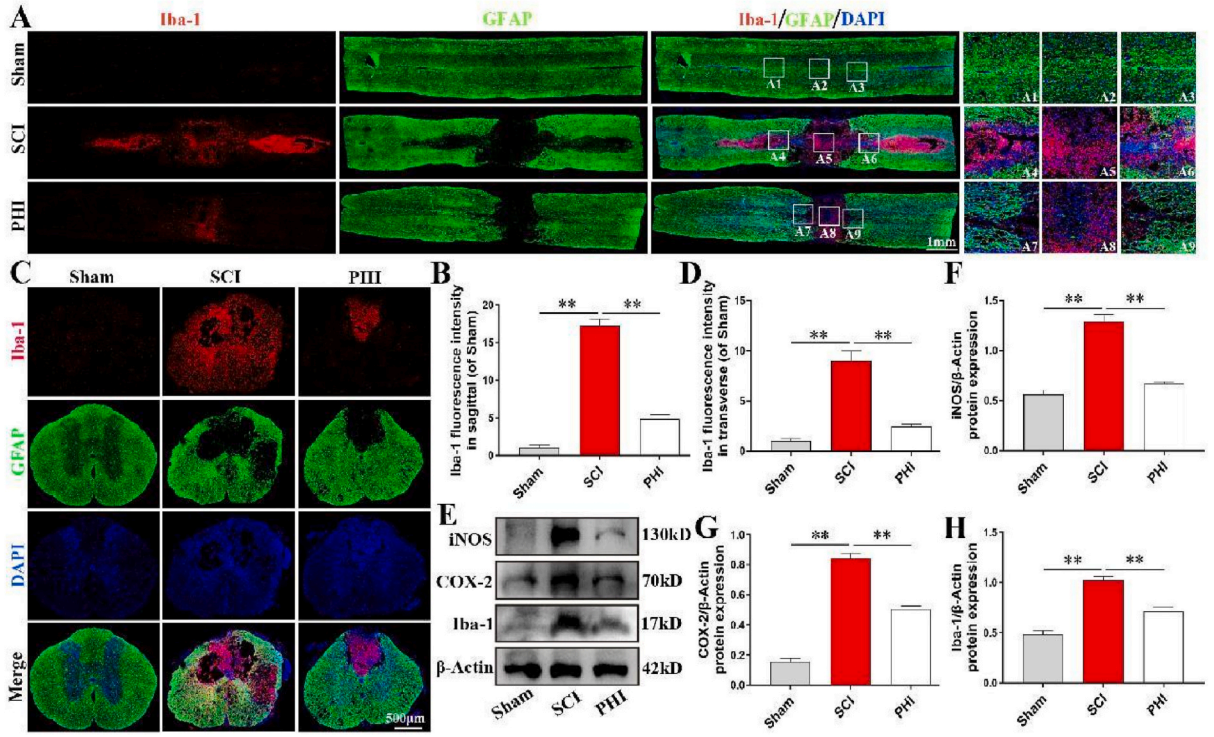

Figure 2. The administration of PHI significantly suppressed the inflammatory response following SCI in rats. (**A, B**) Iba-1 and GFAP staining in longitudinal sections of spinal cord in rats from each group at 7 days post-injury, Scale bar = 1 mm. (**C, D**) Iba-1 and GFAP staining results in transverse sections of spinal cord in rats from each group at 7 days post-injury, Scale bar = 500 μm. (**E–H**) iNOS, COX-2, and Iba-1 protein levels in rats from each group at 7 days post-injury. n = 3 per group for immunofluorescence staining and n = 3 per group for WB. Data are presented as mean ± SD. *P < 0.05 and **P < 0.01.

these findings indicate that PHI exerts a substantial anti-inflammatory effect by suppressing the expression of inflammatory mediators and mitigating microglial hyperactivation.

3.3. PHI mitigated neuronal death and enhanced axonal regeneration following SCI

Next, we investigated the neuroprotective effects of PHI *in vivo*. Nissl staining indicated that the loss of abdominal motor neurons was attenuated by PHI treatment (Fig. 3A). Furthermore, WB analysis of the SCI region revealed a similar trend in the expression of NeuN (Fig. 3B and C; $p < 0.01$). Bcl-xL, a member of the Bcl-2 family, is associated with mitochondrial anti-apoptotic functionality. Immunofluorescence staining and WB revealed significantly higher expression levels of Bcl-xL in the PHI group (Fig. 3D–G; $p < 0.01$). These findings suggest that PHI effectively inhibited neuronal apoptosis in the injured spinal cord.

We also investigated the potential impact of PHI on axonal regeneration after SCI. Immunofluorescence analysis srevealed the presence of MAP2-positive cells, representing neurons that exhibited a shorter distance from the center of the injury site (dashed yellow line) in animals receiving PHI treatment (Fig. 4A and B; $p < 0.05$). When investigating axonal regeneration, we observed a greater presence of neurofilaments within GAP43-positive cells at the injury site in rats from the PHI-treated group. Notably, these neurofilaments penetrated the glial scar at the site of injury (Fig. 4C and D; $p < 0.05$). WB analysis further indicated a significant elevation in the expression levels of GAP43 and MAP-2 proteins in the PHI treatment group (Fig. 4E–G; $p < 0.05$); these findings were consistent with results arising from immunofluorescence analysis. These results indicate that PHI treatment contributes to the alleviation of neuronal loss and the stimulation of axonal repair following SCI, thereby enhancing the recovery of motor function.

3.4. PHI suppressed the release of pro-inflammatory cytokines in activated microglia

To investigate the mechanism by which PHI mitigates neuroinflammation, we next constructed a model of neuroinflammation using activated BV2 cells. The chemical structure of PHI is shown in Fig. 5A. Cell viability assays further revealed that PHI did not exert significant toxic effects on microglia at concentrations below 100 μg/ml. Microglia that had been pretreated with PHI exhibited attenuation of the amoeba-like morphological changes in microglia induced by LPS stimulation (Fig. 5B). qPCR results further demonstrated that PHI inhibited the expression of inflammatory mediators (IL-1β, TNF-α, COX-2 and iNOS) in activated microglial cells in a dose-dependent manner (Fig. 5D–G), thus indicating that PHI exhibited anti-inflammatory effects. The double immunostaining of CD11b and Iba-1 revealed a similar trend. Pretreatment with PHI significantly inhibited activated microglial cells in a dose-dependent manner (Fig. 5H and I). In addition, WB analysis demonstrated that PHI suppressed the expression of iNOS and COX-2 proteins induced by LPS in a dose-dependent manner (Fig. 5J–L). Collectively, these findings highlighted the substantial anti-neuroinflammatory role of PHI in ameliorating excessive microglial activation and the production of inflammatory mediators.

3.5. PHI inhibited the activation of BV2 cell-mediated neuronal apoptosis

We investigated the ability of PHI to inhibit the activation of microglial cells and suppress the production of related inflammatory mediators. These findings support the significant efficacy of PHI in the inhibition of microglial polarization and inflammation, and its ability to create a permissive environment for neuronal survival [23]. In conjunction with our *in vivo* results, the administration of PHI suffering from SCI exhibited a significantly lower rate of neuronal apoptosis in spinal cord tissue when compared to the SCI group.

Next, we investigated the impact of PHI on neuronal cell apoptosis. Initially, we evaluated the direct impact of PHI on VSC4.1 neuronal

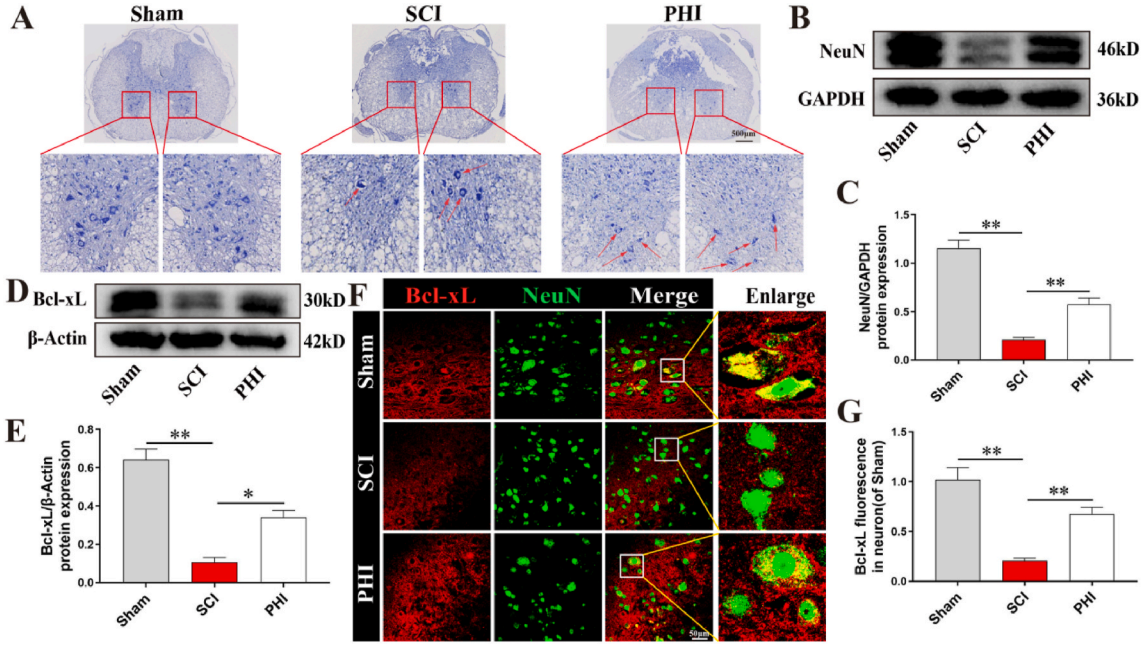

Figure 3. PHI alleviated apoptosis levels in neurons after SCI.
(**A**) The assessment of neuronal survival in transverse sections 7 days post-injury by Nissl staining, scale bar = 500 μm. (**B, C**) Detection and quantification of the levels of neuronal protein NeuN in spinal cord tissues from each group 7 days post-injury. (**D, E**) Detection and quantification of the expression levels of Bcl-xL in spinal cord tissues from each group 7 days post-injury. (**F**) Double immunofluorescence staining of Bcl-xL and NeuN in longitudinal tissue sections 7 days post-injury, Scale bar = 15 μm. (**G**) Quantitative analysis of Bcl-xL fluorescence intensity in neurons. n = 3 per group for histology analysis and n = 3 per group for WB. Data are presented as mean ± SD. *P < 0.05 and **P < 0.01.

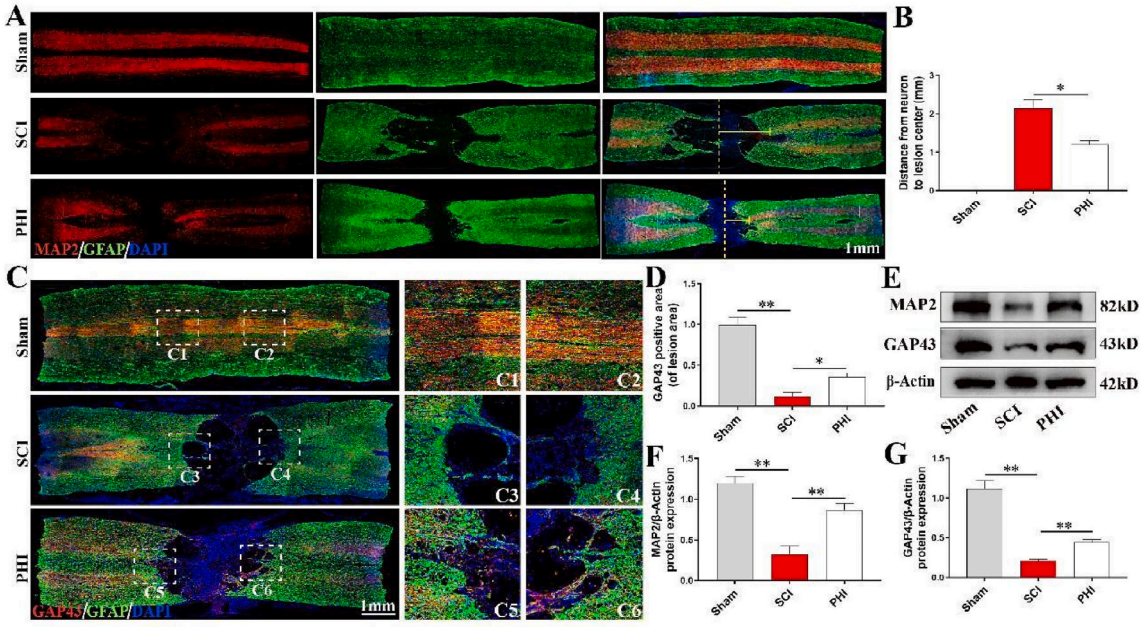

Figure 4. PHI promoted axonal regeneration after SCI.
(**A**) At 42 days post-injury, the PHI group exhibited shorter distances of neurons closest to the injury center, as indicated by GFAP (green) and MAP-2 (red), scale bar = 1 mm. (**B**) Quantitative bar graph showing the distances of neurons to the lesion center, as shown in panel **A**. (**C**) At 42 days post-injury, the PHI group featured a larger number of axonal markers passing through the lesion area, as labeled by GFAP (green) and GAP43 (red), scale bar = 1 mm. (**D**) Quantitative bar graph showing the GAP43 fluorescence intensity from **C**. (**E–G**) WB images and quantification showing the expression levels of MAP-2 and GAP43 proteins in the lesion area. n = 3 per group for immunofluorescence staining and n = 3 per group for WB. Data are shown as mean ± SD. *P < 0.05 and **P < 0.01. (For interpretation of the references to color in this figure legend, the reader is referred to the Web version of this article.)

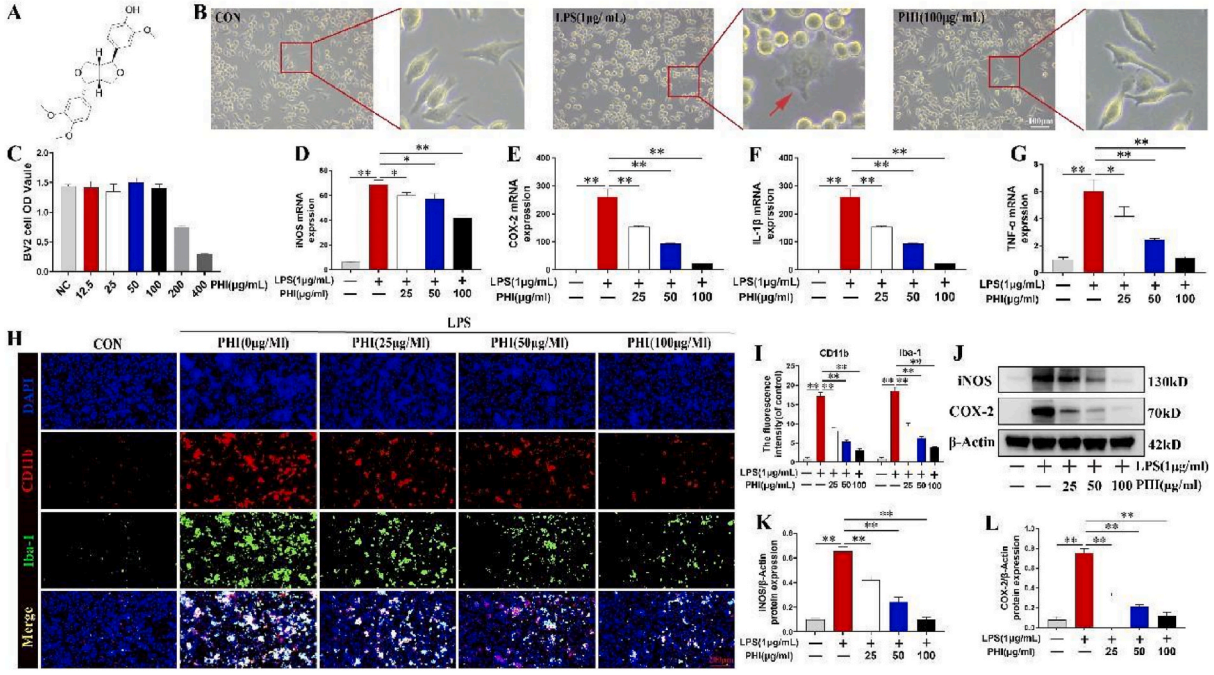

Figure 5. PHI suppressed the release of pro-inflammatory mediators in lipopolysaccharide-activated microglia. (**A**) Chemical structure of PHI. (**B**) PHI inhibited morphological changes in activated microglia, scale bar = 100 μm. (**C**) Impact of different concentrations of PHI on the viability of BV2 cells, as determined by CCK-8. (**D–G**) RT-qPCR analysis of the expression of inflammatory markers, iNOS, COX-2, TNF-α, and IL-1β, in different groups. (**H, I**) Immunofluorescence staining and corresponding bar graph quantification data demonstrating the expression levels of CD11b and Iba-1 in microglia for each experimental group, scale bar = 200 μm. (**J–L**) The effect of a gradient of PHI concentrations on iNOS and COX-2 protein levels in microglia. n = 3 per group for immunofluorescence staining and n = 3 per group for WB. Data are shown as mean ± SD. *P < 0.05 and **P < 0.01.

cells. By employing the Transwell cell co-culture method, VSC4.1 neuronal cells were pretreated with a gradient of PHI concentrations and then co-cultured with polarized BV2 cells. When VSC4.1 neuronal cells were directly exposed to PHI, there was no difference in the apoptosis rate when compared between the untreated group and the VSC4.1 neuronal cells that had been pretreated with a gradient of PHI concentrations following stimulation with inflammatory mediators, as revealed by Calcein-AM/PI double staining. These results suggested that PHI cannot directly inhibit apoptosis in VSC4.1 neuronal cells (Fig. 3S).

Building upon the indication that PHI can inhibit BV2 microglial cells from producing inflammatory mediators, we proceeded to investigate whether the ability of PHI to inhibit apoptosis in VSC 4.1 neuronal cells depended on its action on BV2 microglial cells, as illustrated in Fig. 6A. When VSC 4.1 cells were co-cultured with LPS-activated microglia, they exhibited significant morphological changes, including axonal contraction. Nevertheless, the pretreatment of BC2 cells with PHI prior to LPS exposure partially mitigated these morphological changes when co-cultured with VSC 4.1 cells, thus resulting in longer synaptic structures (Fig. 6B). Consistent with WB results, the PHI intervention group exhibited a significant increase in the expression of Bcl-xL protein

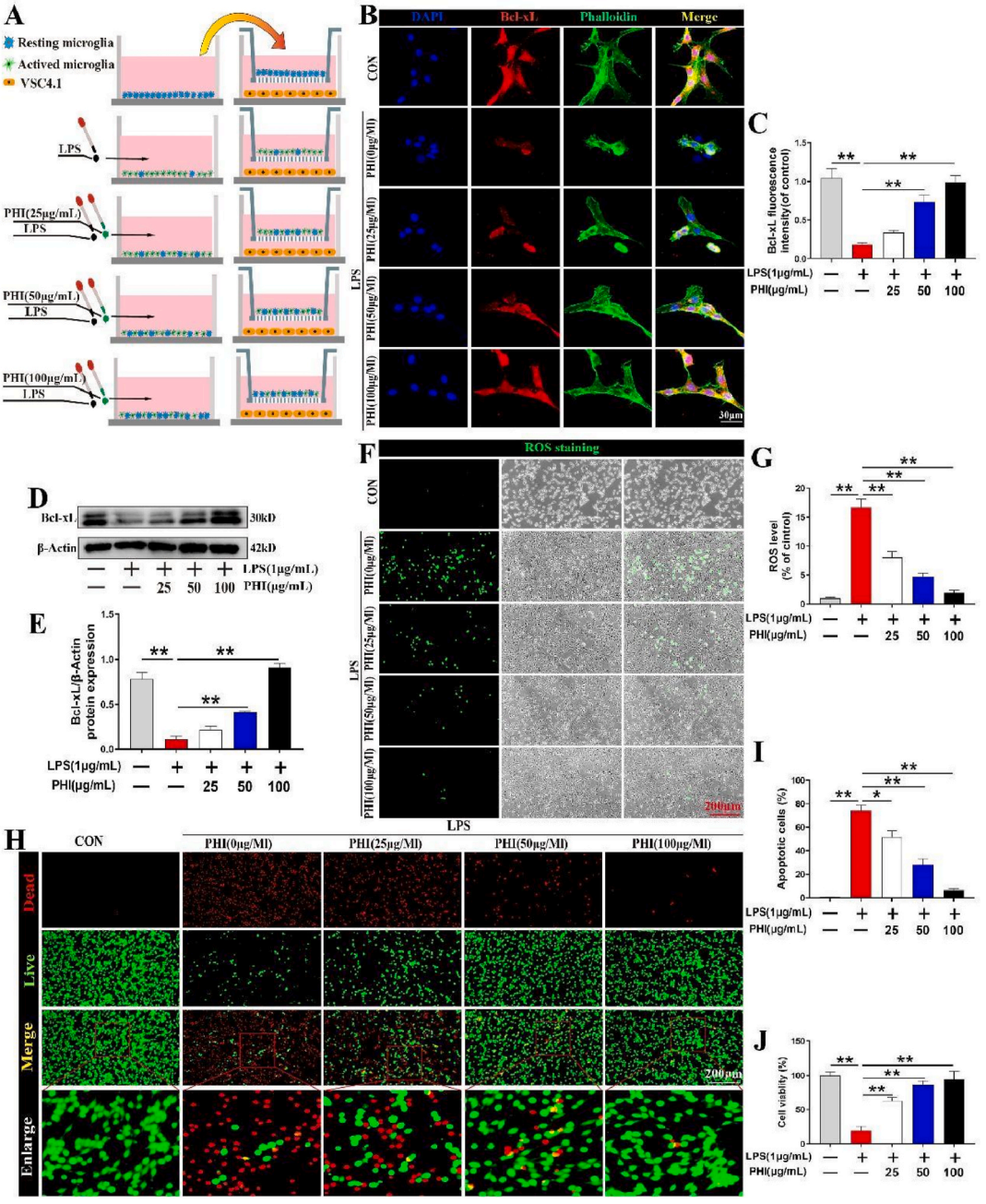

Figure 6. PHI exerted neuroprotective effects against neurotoxicity mediated by activated microglia. (**A**) Schematic representation of BV2 microglial cells and VSC4.1 neuronal cells following co-culture. (**B, C**) Expression levels of Bcl-xL and Phalloidin in VSC4.1 cells, scale bar = 30 μm. (**D, E**) WB images and quantification showing the levels of Bcl-xL protein in VSC4.1 cells. (**F**) Detection of intracellular ROS in VSC4.1 cells, scale bar = 200 μm. (**G**) Quantitative analysis of the proportion of ROS-positive VSC4.1 cells in each group. (**H**) Double labeling revealing the proportions of live cells (green) and dead VSC4.1 cells (red) in each group, as determined by Calcein-AM/PI, scale bar = 200 μm. (**I, J**) Quantitative analysis of the proportions of dead and live VSC4.1 cells. n = 3 per group for WB. Data are presented as means ± SD. *P < 0.05 and **P < 0.01. (For interpretation of the references to color in this figure legend, the reader is referred to the Web version of this article.)

(Fig. 6B–E; $p < 0.05$). Next, we investigated the impact of PHI on neuronal apoptosis using a live/dead double staining kit (Calcein-AM/PI). Analysis demonstrated that PHI had the ability to counteract the neuronal apoptosis induced by activated microglia (Fig. 6H–J; $p < 0.01$).

ROS refer to a class of oxidative molecules including superoxide anions, hydrogen peroxide, and hydroxyl radicals [24]. Elevated levels of ROS are known to induce OS, thus leading to oxidative damage in cells [25]. We observed a dose-dependent reduction in ROS levels in VSC 4.1 cells when co-cultured with BV2 cells treated with different concentrations of PHI, as detected by a ROS assay kit (Fig. 6F and G; $p < 0.01$). The mitochondrial membrane potential ($\Delta\Psi m$ or MMP) represents the electrochemical gradient formed by uneven proton distribution across the inner mitochondrial membrane [26]. A reduction in MMP is a hallmark event of cell apoptosis [27]. Hence, we proceeded with additional assessments to investigate whether the neuroprotective effects of PHI are linked to the stabilization of mitochondrial function. We used a JC-1 assay kit and observed that PHI treatment led to a dose-dependent restoration of MMP in co-cultured VSC 4.1 cells (Fig. 4S; $p < 0.05$). This observation aligns with the trend observed for ROS indicators following the pretreatment of VSC 4.1 cells with PHI (Fig. 6F; $p < 0.05$). These findings confirmed that PHI exhibits strong neuroprotective effects by inhibiting the neuronal apoptosis mediated by activated microglia, as well as the mitigation of mitochondrial dysfunction and a reduction in ROS production.

PHI directly targeted the TLR4 protein and inhibited inflammatory factors by inhibiting the expression of TLR4.

Next, we investigated the molecular mechanisms underlying the ability of PHI to suppress neuroinflammation in microglia. To do this, we conducted bioinformatic analysis to identify potential targets of PHI. By searching the Swiss Target Prediction online database, 193 proteins were predicted to be targets of PHI. Simultaneously, we identified 106 common targets from a pool of 3727 proteins associated with inflammatory diseases sourced from the GeneCards, NCBI, and OMIM databases (Fig. 7A–D). We performed KEGG pathway enrichment analyses for overlapping targets. These were then sorted by correlation pathways (Fig. 7B). Our investigation revealed the involvement of toll-like receptor signaling pathways in the modulation of inflammatory responses mediated by microglia, and that this pathway ranked the highest among all inflammation-related pathways. TLR4 was identified as a central core target by both topological and MCODE clustering analyses (Fig. 7D). Furthermore, the core target identified by clustering, TLR4, is also an important molecule within the toll-like receptor signaling pathway. We applied AutoDock Vina for the molecular docking of PHI (PubChem CID: 3083590) with the TLR4 protein (protein number: 4G8A) and observed that PHI exhibited binding capability to the active pocket of TLR4. The predominant conformation was chosen for subsequent docking analysis, and the binding energy generated by interaction was calculated to be −6.7 kcal/mol (Fig. 7E and F).

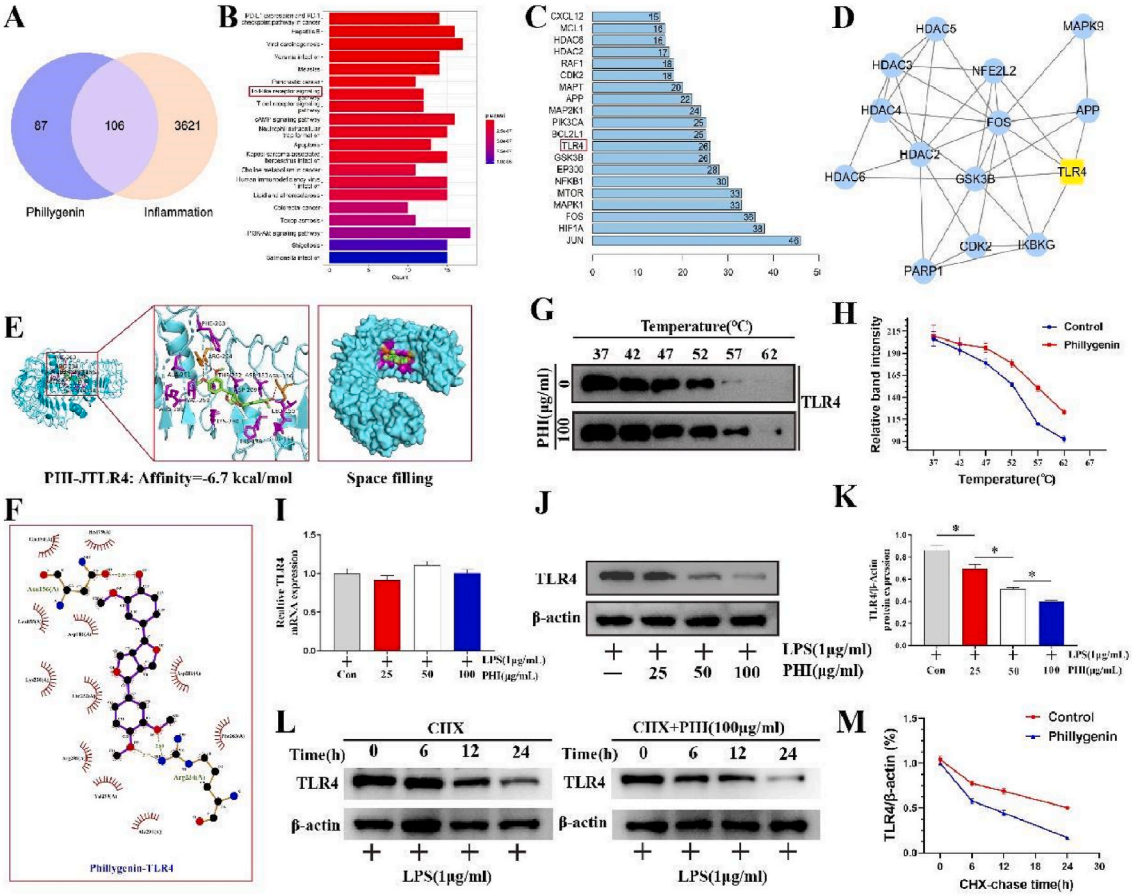

Figure 7. PHI can bind to TLR4 and affect its translation. (**A**) Intersection of PHI target proteins and inflammation-related proteins, revealing 106 common targets. (**B**) KEGG pathway enrichment analysis of common targets related to drugs and diseases. (**C, D**) Common targets were imported into Cytoscape software and key proteins were identified by topological analysis and MCODE cluster analysis. (**E, F**) Molecular docking of PHI molecules and TLR4 protein by AutoDock Vina. The spatial binding model demonstrates PHI binding within the TLR4 binding pocket. (**G, H**) CETSA quantitative analysis showing the thermal stability of TLR4 protein with PHI treatment (100 μg/mL) or without treatment. (**I**) qRT-PCR analysis of TLR4 mRNA levels in activated BV2 cells treated with PHI. (**J, K**) Assessment of TLR4 protein expression in activated BV2 cells treated with gradient concentrations of PHI, followed by quantitative analysis. (**L, M**) Activated BV2 cells were treated with CHX, with or without PHI treatment. Protein expression of TLR4 was analyzed by WB and quantified. n = 3 per group for WB. Results are shown as mean ± SD. *$P < 0.05$ and **$P < 0.01$.

qRT-PCR further revealed that PHI treatment had no impact on the mRNA levels of TLR4 in BV2 cells, thus suggesting that PHI did not influence the transcription of TLR4. However, PHI exhibited a dose-dependent inhibition of TLR4 protein expression in BV2 cells (Fig. 7J). Cellular thermal shift assays (CETSAs) with BV2 cells further demonstrated that PHI improved the thermal stability of TLR4, thus indicating that PHI might be responsible for the interaction with TLR4 (Fig. 7G and H). Furthermore, we employed cycloheximide (CHX), a translational inhibitor, to treat BV2 cells, in an attempt to investigate whether PHI had an impact on the stability of the TLR4 protein. WB analysis revealed that CHX led to the time-dependent inhibition of TLR4 protein expression in BV2 cells. Notably, the inhibitory effects of CHX on TLR4 protein expression were significance enhanced when cells were co-treated with PHI (Fig. 7L). These findings strongly suggested that PHI affected TLR4 protein translation and stability rather than influencing gene transcription.

3.6. PHI inhibited inflammatory factors by inhibiting the expression of TLR4

To determine whether PHI induces inflammatory factors via the inhibition ofTLR4, the levels of TLR4 were upregulated by the transfection of BV2 cells with PLV3-CMV-TLR4. WB analysis revealed a significant upregulation in the protein levels of the inflammatory cytokines iNOS and COX-2, both of which were inhibited by PHI (Fig. 8A–D). The mRNA levels of iNOS, COX-2, IL-1β, and TNF-α were inhibited by PHI in BV2 cells overexpressing TLR4 (Fig. 8E–H). In addition, we further evaluated the expression of Iba-1 protein by immunofluorescence staining in BV2 cells overexpressing TLR4 and found that Iba-1 protein was downregulated by PHI (Fig. 8I). Collectively, these data suggested that PHI downregulated inflammatory factors by targeting TLR4.

3.7. PHI induced the NF-κB signaling pathway by inhibiting the expression of TLR4

In BV2 microglia, WB analysis revealed that the levels of TLR4 and MYD88 proteins increased significantly in response to LPS treatment, as confirmed by WB analysis. Notably, this effect was effectively ameliorated by pretreatment with PHI (Fig. 9A–C). Subsequently, we investigated whether PHI modulated LPS-induced neuroinflammation via the NF-κB pathway. WB analysis revealed that LPS treatment significantly increased the phosphorylation levels of P65 and IκBα in BV2 microglia, which were effectively attenuated by PHI pretreatment (Fig. 9D–F). To further investigate the role of the NF-κB signaling pathway in the PHI-induced reduction of pro-inflammatory mediator release, microglia were pretreated with PHI (0 or 100 μg/ml) prior to exposure to LPS. Cells were incubated with or without the NF-κB pathway inhibitor pyrrolidinedithiocarbamate (PDTC, 50 μmol/L) for 2 h. As demonstrated in Fig. 9G–I, the therapeutic combination of PDTC and PHI significantly reduced the phosphorylation of P65 and IκBα when compared with PDTC or PHI monotherapy ($p < 0.05$). Similarly, the simultaneous administration of PDTC and PHI led to a significant reduction in the levels of iNOS and COX-2 proteins when compared to individual treatments with PDTC or PHI alone (Fig. 9J–L). To further investigate the effect of PHI on the subcellular localization of p65 in activated microglia, we next conducted immunofluorescence staining. Following LPS

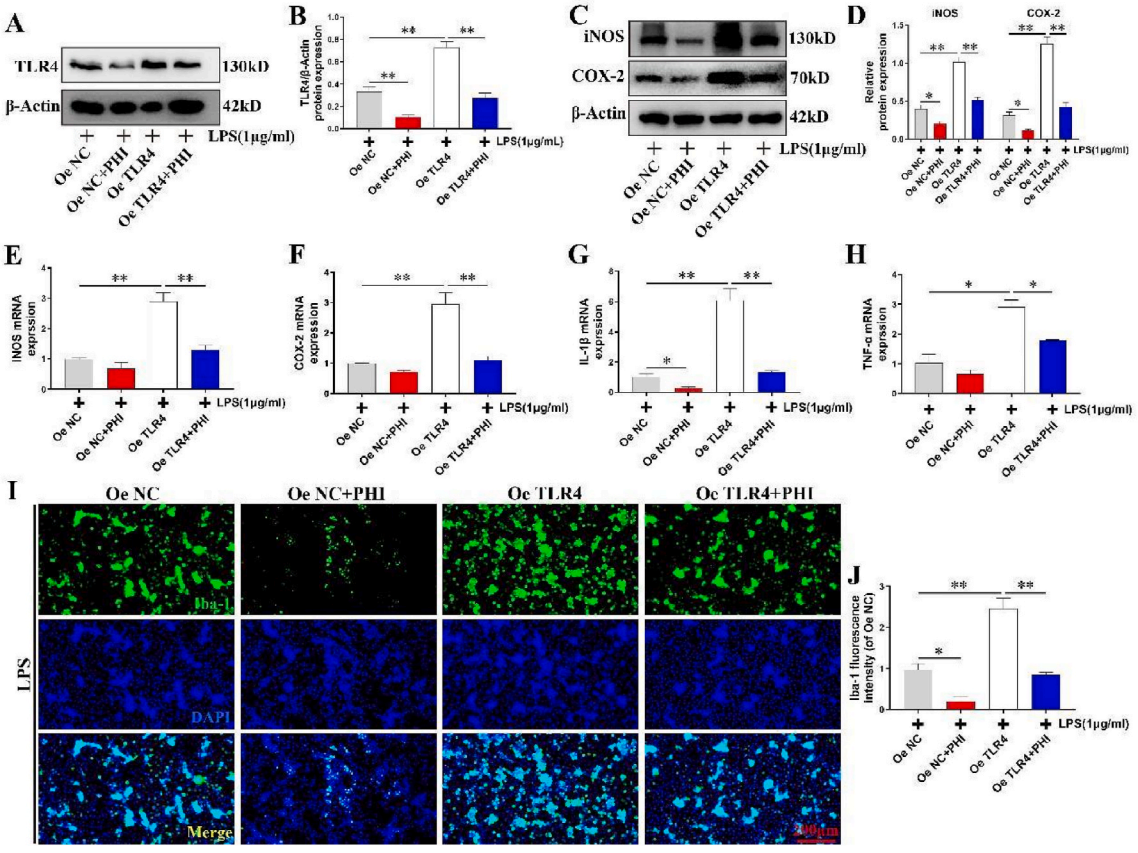

Figure 8. PHI suppressed neuroinflammation by inhibiting TLR4 expression. BV2 cells were infected with PLV3-CMV-TLR4 or empty vector; after infection, cells were treated with 100 μg/mL PHI for 12 h. (**A, B**) Protein expression of TLR4 in each group following PHI treatment. (**C, D**) The expression of inflammatory markers (iNOS and COX-2 proteins) in each group following PHI treatment. (**E–H**) mRNA levels of inflammatory factors in each group following PHI treatment, as determined by qRT-PCR. (**I, J**) The expression levels of Iba-1 in microglial cells in each group after PHI treatment, scale bar = 200 μm. n = 3 per group for WB. Data are shown as mean ± SD. *P < 0.05 and **P < 0.01.

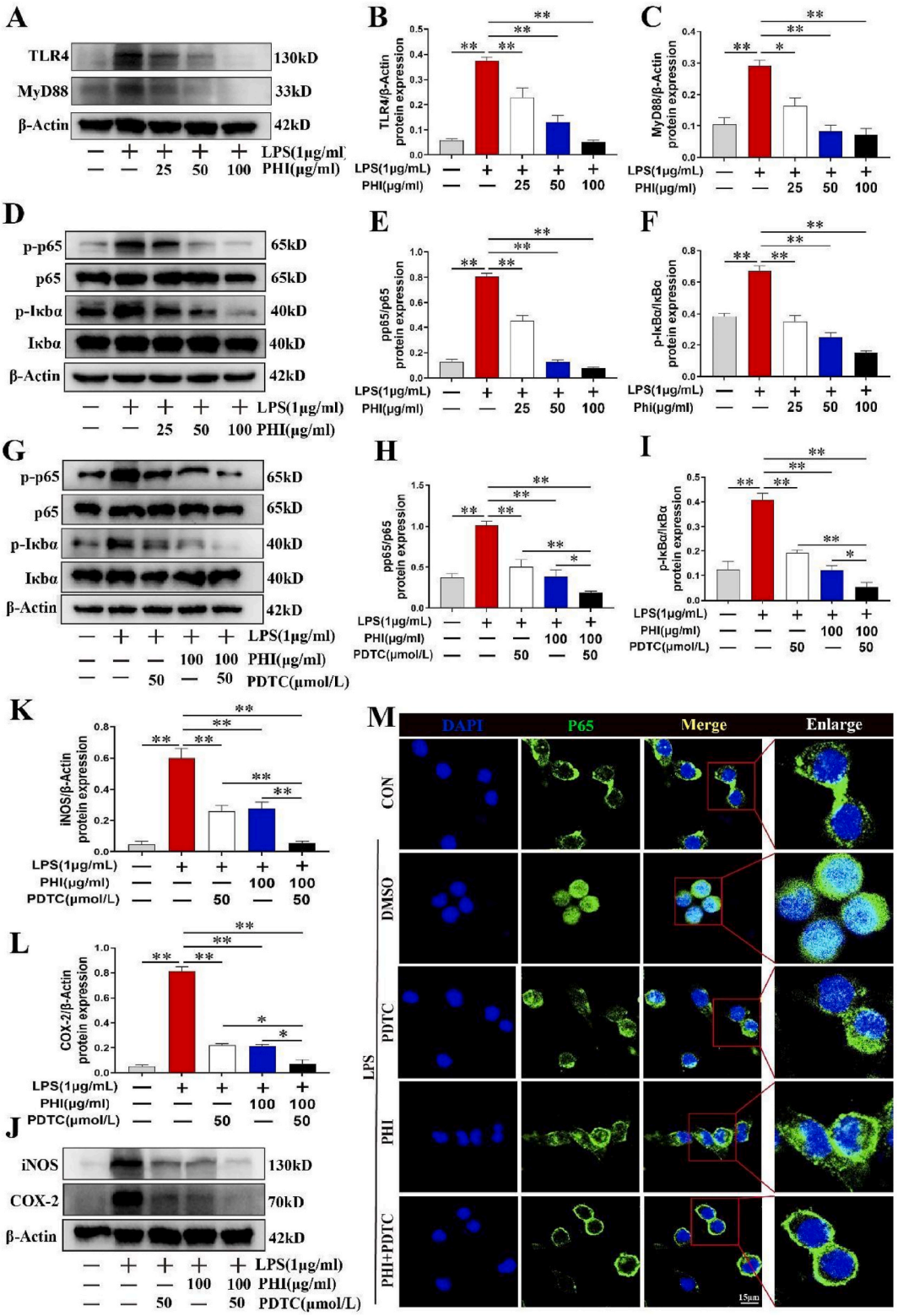

Figure 9. PHI suppressed LPS-induced neuroinflammatory response in microglial cells by targeting TLR4 to inhibit the NF-κB signaling pathway. (A–C) WB images and quantification depicting the expression levels of TLR4 and MyD88 in microglial cells after gradient PHI treatment. (D–F) WB images and quantification of the expression levels of p-p65, p65, p-IκBα, and IκBα in microglial cells after gradient PHI treatment. (G–I) WB images and quantification showing the expression levels of p-p65, p65, p-IκBα, and IκBα in microglial cells after treatment with PHI and PDTC. (J–L) WB images and quantification showing the protein expression levels of iNOS and COX-2 after treatment with PHI and PDTC. (M) Immunofluorescence detection of p65 (green fluorescence) cellular localization after treatment with PHI and PDTC, scale bar = 15 μm. n = 3 per group for immunofluorescence staining, n = 3 per group for WB. Data are presented as mean ± SD. *P < 0.05 and **P < 0.01. (For interpretation of the references to color in this figure legend, the reader is referred to the Web version of this article.)

treatment, the phosphorylation of p65 increased, thus resulting in the enhanced translocation of p65 into the cell nuclei. However, PHI pretreatment effectively attenuated the LPS-induced elevation in p65 nuclear translocation. Additionally, the combination of PDTC and PHI demonstrated a more pronounced inhibitory effect on p65 nuclear translocation (Fig. 9M). These findings collectively indicated that the anti-inflammatory action of PHI was mediated by its interaction with the TLR4/MYD88/NF-κB pathway.

4. Discussion

Neuroinflammation is a crucial pathophysiological response to SCI and plays a significant role in its development [28,29]. An important component of secondary injury is microglial activation, which results in OS and the onset of neuroinflammation [30,31]. PHI, the primary bioactive compound in forsythia, is known to exert a range of biomedical effects and demonstrates potent anti-inflammatory activity [18]. The biological effects of PHI on SCI remain unclear. In this study, we identified PHI as a potent agent for inhibiting the detrimental progression of SCI. Furthermore, our research demonstrated that PHI could enhance the restoration of neurological function in rats suffering from SCI. Furthermore, we demonstrated that PHI effectively reduced the inflammatory response and neuronal apoptosis in spinal cord tissue in a rat model of SCI. Subsequent *in vitro* investigations further substantiated that PHI effectively attenuated neuroinflammation mediated by activated microglia. The effects of PHI on the inhibition of neuroinflammation and neuronal apoptosis were confirmed by the microglial activation and co-culture assay model. Moreover, TLR4 was predicted and confirmed as the target protein for PHI. By transfecting cells with TLR4 overexpression plasmids, the anti-inflammatory properties of PHI were partially reversed.

Recent studies have increasingly demonstrated the therapeutic potential of bioactive compounds derived from Chinese herbal medicines for SCI [32,33]. PHI is the principal active ingredient of forsythia, a traditional medicinal plant [34]. PHI offers several pharmacological benefits, including hepatoprotective, cardiovascular protective, and antioxidant properties, all with low levels of systemic toxicity [18]. In a previous study, Zhang et al. [35] demonstrated that PHI was able to ameliorate osteoarthritis by inhibiting the inflammation of chondrocytes in mice. In another study, Zhou et al. [19] demonstrated that PHI alleviated non-alcoholic fatty liver disease by enhancing TFEB-mediated lysosome biogenesis and by promoting lipophagy. In addition, PHI was reported to exhibit a significant anti-RSV effect by inhibiting the PI3K/AKT signaling pathway [36]. However, the specific mechanisms responsible for the anti-inflammatory and neuroprotective effects of PHI in SCI have yet to be elucidated.

In the present research, we found that PHI efficiently inhibited microglial activation and reduced the release of inflammatory mediators. The treatment of SCI with PHI reduced neuroinflammation and neuronal apoptosis, ultimately promoting the recovery of SCI. These data suggest that PHI can effectively impede the progression of SCI, thus identifying a new functional application for this medicine. Over recent years, an increasing array of natural compounds have been identified as potential agents for the treatment of SCI. One example is alpinetin, the main active ingredient in Alpinia katsumadai Hayata, which has been reported to be beneficial for patients recovering from SCI [37]. Our present study is the first to suggest that PHI represents a novel agent for the improvement of SCI.

Secondary injury develops within minutes to weeks following initial SCI [38] and is characterized by an inflammatory response involving neutrophil infiltration and microglial activation [29] that leads to the release of ROS and pro-inflammatory cytokines [9,39]. The stabilization of MMP is essential for maintaining normal functionality in neuronal cells [40,41]. Furthermore, uncontrolled neuroinflammation is a significant contributor to increased apoptosis and dysfunction in various essential cell types, thereby exacerbating the neurological consequences of SCI [42]. Microglia, the primary resident immune cells of the CNS [43,44], respond to diverse forms of nerve injury and play a pivotal role in neuroinflammation in the CNS [45]. In the current study, we highlight the role of PHI as a novel anti-inflammation agent for activated microglia. In VSC4.1 neuronal cells, PHI treatment induced the reversal of ROS production and MMP, ultimately reducing apoptosis. These findings indicated that PHI exerted an anti-inflammatory effect on activated microglia, thus demonstrating the critical role of PHI in the modulation of neuroinflammation and neuronal apoptosis during the development of SCI.

TLR4 is a pivotal component within the toll-like receptor signaling pathway and plays a significant role in the pathophysiology of neurodegenerative diseases [46,47]. Notably, previous studies have shown that TLR4 inhibitors can effectively halt the elevation of pro-inflammatory protein levels following ischemic brain injury [48]. Furthermore, the NF-κB pathway is increasingly being acknowledged as a central player in the neuroinflammation mediated by activated microglia, making this pathway a promising therapeutic target for mitigating neuroinflammatory responses [49,50]. Typically, LPS is recognized by TLR4, triggering a subsequent signaling cascade [51]. This reaction causes TLR4 to engage with its downstream partner, MyD88, which, in turn, activates the NF-κB-related signaling pathway in a MyD88-dependent manner. This activation step facilitates the release of inflammatory cytokines and chemokines, including tumor necrosis factor-α (TNF-α) and IL-1β [46,52,53]. In the present study, we identified TLR4 as the primary target of PHI. Molecular docking analysis revealed that PHI binds effectively to the active pocket of TLR4 to inhibit both TLR4 and NF-κB phosphorylation in activated microglia. Importantly, this inhibitory effect did not influence the total protein levels of P65 and IκBα. Additionally, the suppression of NF-κB pathway activity by PDTC substantially attenuated the LPS-induced P65 and IκBα phosphorylation levels, as well as the protein expression of iNOS and COX-2. Furthermore, when PDTC and PHI were used in combination, we observed a synergistic effect in the inactivation of the NF-κB pathway and the suppression of neuroinflammation. Collectively, these findings present a novel mechanism by which PHI targets TLR4, reducing its protein expression, and subsequently deactivating the NF-κB pathway, ultimately exerting potent anti-inflammatory effects.

5. Conclusions

In this study, we acquired compelling evidence to support the fact that PHI can efficiently prevent microglial activation and the subsequent neuroinflammatory response. This action is achieved by targeting TLR4 and inhibiting the NF-κB pathway following SCI. Furthermore, this inhibition mitigates neurotoxic factor-induced neuronal apoptosis, ultimately promoting axonal regeneration and facilitating motor function recovery following SCI (Fig. 10). Collectively, these findings provide a novel mechanism by which PHI mitigates the progression of SCI, thus suggesting its potential as a therapeutic agent for SCI.

Funding information

This work was supported by Jiangxi Provincial Natural Science Foundation-Key Project [grant number 20232ACB206023].

Author contributions

Yu Zhang, Shining Xiao, and Zhili Liu were responsible for experimental design. Yu Zhang and Shining Xiao drafted the manuscript. Yu Zhang, Shining Xiao, Dan Fan, Geliang Yao, and Shu'e Hong conducted the experiments and analyzed the data. Jiaming Liu revised the manuscript. Zhili Liu contributed to experimental design, data analysis, and interpretation. All authors reviewed and approved the final manuscript.

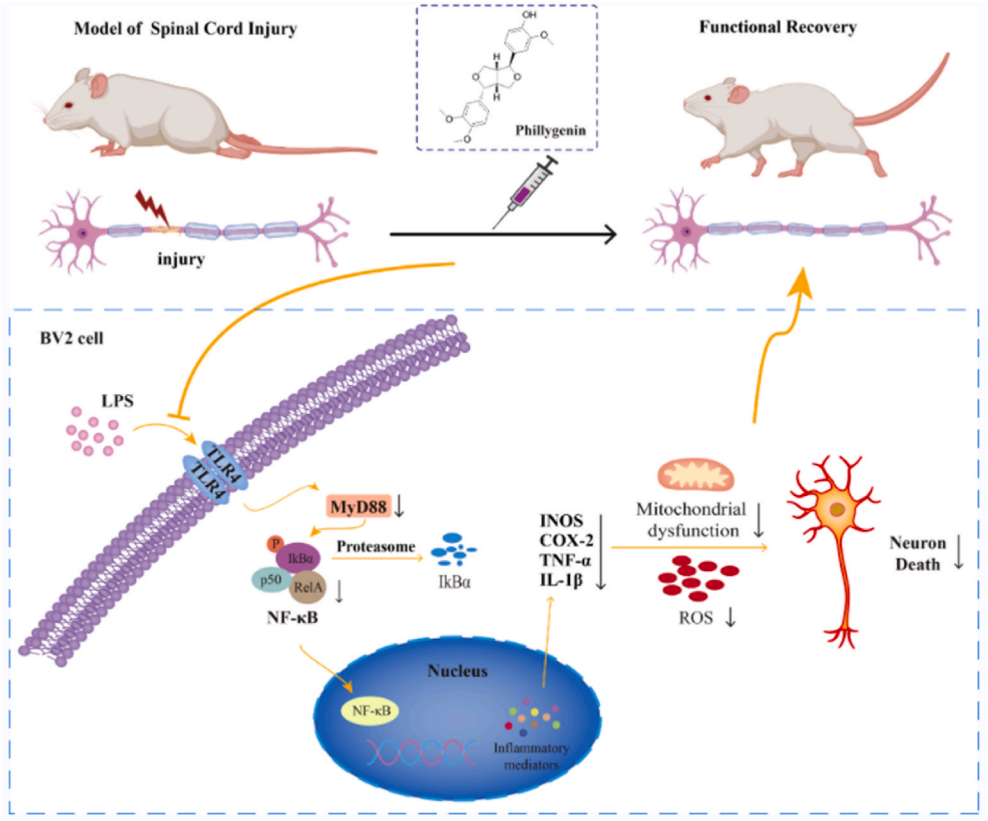

Figure 10. Mechanism of action of PHI for the treatment of SCI.
PHI alleviated the inflammation and neurotoxicity caused by activated microglial cells by targeting TLR4 and inhibiting the NF-κB pathway, ultimately promoting functional recovery in rats with SCI.

Ethics statement

All animal experiments were approved by the Ethics Committee of the First Affiliated Hospital of Nanchang University (CDYFY-IACUC-202306QR039).

Data availability statement

The datasets analyzed during the current study are available from the corresponding author on reasonable request.

Declaration of competing interest

The authors declare that we have no known competing financial interests or personal relationships that could have appeared to influence the work reported in this paper.

Acknowledgements

We would like to extend our thanks to Nanshan Zhong, Ning Liu, Yujia Zeng and Ke Huang for their assistance.

Appendix A. Supplementary data

Supplementary data to this article can be found online at https://doi.org/10.1016/j.jot.2024.07.013.

References

[1] Gilbert EAB, Lakshman N, Lau KSK, Morshead CM. Regulating endogenous neural stem cell activation to promote spinal cord injury repair. Cells 2022;11(5) [eng].
[2] Hu X, Xu W, Ren Y, Wang Z, He X, Huang R, et al. Spinal cord injury: molecular mechanisms and therapeutic interventions. Signal Transduct Targeted Ther 2023;8(1):245 [eng].
[3] Hou Y, Luan J, Huang T, Deng T, Li X, Xiao Z, et al. Tauroursodeoxycholic acid alleviates secondary injury in spinal cord injury mice by reducing oxidative stress, apoptosis, and inflammatory response. J Neuroinflammation 2021;18(1):216 [eng].
[4] Bretheau F, Castellanos-Molina A, Bélanger D, Kusik M, Mailhot B, Boisvert A, et al. The alarmin interleukin-1α triggers secondary degeneration through reactive astrocytes and endothelium after spinal cord injury. Nat Commun 2022;13(1):5786 [eng].
[5] Li Y, Lei Z, Ritzel RM, He J, Li H, Choi HMC, et al. Impairment of autophagy after spinal cord injury potentiates neuroinflammation and motor function deficit in mice. Theranostics 2022;12(12):5364–88 [eng].
[6] Shao A, Tu S, Lu J, Zhang J. Crosstalk between stem cell and spinal cord injury: pathophysiology and treatment strategies. Stem Cell Res Ther 2019;10(1):238 [eng].
[7] Chio JCT, Xu KJ, Popovich P, David S, Fehlings MG. Neuroimmunological therapies for treating spinal cord injury: evidence and future perspectives. Exp Neurol 2021;341:113704 [eng].
[8] Yang B, Zhang F, Cheng F, Ying L, Wang C, Shi K, et al. Strategies and prospects of effective neural circuits reconstruction after spinal cord injury. Cell Death Dis 2020;11(6):439 [eng].
[9] Zrzavy T, Schwaiger C, Wimmer I, Berger T, Bauer J, Butovsky O, et al. Acute and non-resolving inflammation associate with oxidative injury after human spinal cord injury. Brain 2021;144(1):144–61 [eng].
[10] Liu H, Zhang J, Xu X, Lu S, Yang D, Xie C, et al. SARM1 promotes neuroinflammation and inhibits neural regeneration after spinal cord injury through NF-κB signaling. Theranostics 2021;11(9):4187–206 [eng].
[11] Liu Z, Yao X, Jiang W, Li W, Zhu S, Liao C, et al. Advanced oxidation protein products induce microglia-mediated neuroinflammation via MAPKs-NF-κB signaling pathway and pyroptosis after secondary spinal cord injury. J Neuroinflammation 2020;17(1):90 [eng].
[12] Li Y, He X, Kawaguchi R, Zhang Y, Wang Q, Monavarfeshani A, et al. Microglia-organized scar-free spinal cord repair in neonatal mice. Nature 2020;587(7835):613–8 [eng].
[13] Li C, Wu Z, Zhou L, Shao J, Hu X, Xu W, et al. Temporal and spatial cellular and molecular pathological alterations with single-cell resolution in the adult spinal cord after injury. Signal Transduct Targeted Ther 2022;7(1):65 [eng].
[14] Li Y, Ritzel RM, Khan N, Cao T, He J, Lei Z, et al. Delayed microglial depletion after spinal cord injury reduces chronic inflammation and neurodegeneration in the

brain and improves neurological recovery in male mice. Theranostics 2020;10(25): 11376–403 [eng].
[15] Rong Y, Ji C, Wang Z, Ge X, Wang J, Ye W, et al. Small extracellular vesicles encapsulating CCL2 from activated astrocytes induce microglial activation and neuronal apoptosis after traumatic spinal cord injury. J Neuroinflammation 2021; 18(1):196 [eng].
[16] Xiao S, Zhang Y, Liu Z, Li A, Tong W, Xiong X, et al. Alpinetin inhibits neuroinflammation and neuronal apoptosis via targeting the JAK2/STAT3 signaling pathway in spinal cord injury. CNS Neurosci Ther 2023.
[17] Zhang L, Xu J, Yin S, Wang Q, Jia Z, Wen T. Albiflorin attenuates neuroinflammation and improves functional recovery after spinal cord injury through regulating LSD1-mediated microglial activation and ferroptosis. Inflammation 2024. https://doi.org/10.1007/s10753-024-01978-8.
[18] Wang C, Wu R, Zhang S, Gong L, Fu K, Yao C, et al. A comprehensive review on pharmacological, toxicity, and pharmacokinetic properties of phillygenin: current landscape and future perspectives. Biomed Pharmacother 2023;166:115410 [eng].
[19] Zhou W, Yan X, Zhai Y, Liu H, Guan L, Qiao Y, et al. Phillygenin ameliorates nonalcoholic fatty liver disease via TFEB-mediated lysosome biogenesis and lipophagy. Phytomedicine 2022;103:154235 [eng].
[20] Xue HH, Li JJ, Li SF, Guo J, Yan RP, Chen TG, et al. Phillygenin attenuated colon inflammation and improved intestinal mucosal barrier in DSS-induced colitis mice via TLR4/src mediated MAPK and NF-κB signaling pathways. Int J Mol Sci 2023;24 (3) [eng].
[21] Li H, Chen M, Yang Z, Wang Q, Wang J, Jin D, et al. Phillygenin, a MELK inhibitor, inhibits cell survival and epithelial-mesenchymal transition in pancreatic cancer cells. OncoTargets Ther 2020;13:2833–42 [eng].
[22] Wang C, Ma C, Fu K, Gong LH, Zhang YF, Zhou HL, et al. Phillygenin attenuates carbon tetrachloride-induced liver fibrosis via modulating inflammation and gut microbiota. Front Pharmacol 2021;12:756924.
[23] Liu Z, Lee H, Dong L, Cheong SH, Lee DS. Fatsia japonica extract exerts antioxidant and anti-neuroinflammatory effects on neuronal cells and a zebrafish model. J Ethnopharmacol 2024;324:117813 [eng].
[24] Yin Z, Wan B, Gong G, Yin J. ROS: executioner of regulating cell death in spinal cord injury. Front Immunol 2024;15:1330678 [eng].
[25] Chandran S, Binninger D. Role of oxidative stress, methionine oxidation and methionine sulfoxide reductases (MSR) in Alzheimer's disease. Antioxidants 2023; 13(1) [eng].
[26] Disha B, Mathew RP, Dalal AB, Mahato AK, Satyamoorthy K, Singh KK, et al. Mitochondria in biology and medicine - 2023. Mitochondrion 2024:101853 [eng].
[27] Zheng Q, Liu H, Gao Y, Cao G, Wang Y, Li Z. Ameliorating mitochondrial dysfunction for the therapy of Parkinson's disease. Small 2024:e2311571 [eng].
[28] Zeng H, Liu N, Yang YY, Xing HY, Liu XX, Li F, et al. Lentivirus-mediated downregulation of α-synuclein reduces neuroinflammation and promotes functional recovery in rats with spinal cord injury. J Neuroinflammation 2019;16 (1):283 [eng].
[29] Hellenbrand DJ, Quinn CM, Piper ZJ, Morehouse CN, Fixel JA, Hanna AS. Inflammation after spinal cord injury: a review of the critical timeline of signaling cues and cellular infiltration. J Neuroinflammation 2021;18(1):284 [eng].
[30] Gao J, Sun Z, Xiao Z, Du Q, Niu X, Wang G, et al. Dexmedetomidine modulates neuroinflammation and improves outcome via alpha2-adrenergic receptor signaling after rat spinal cord injury. Br J Anaesth 2019;123(6):827–38 [eng].
[31] Chen S, Ye J, Chen X, Shi J, Wu W, Lin W, et al. Valproic acid attenuates traumatic spinal cord injury-induced inflammation via STAT1 and NF-κB pathway dependent of HDAC3. J Neuroinflammation 2018;15(1):150 [eng].
[32] Zhang Q, Liu X, Yan L, Zhao R, An J, Liu C, et al. Danshen extract (Salvia miltiorrhiza Bunge) attenuate spinal cord injury in a rat model: a metabolomic approach for the mechanism study. Phytomedicine 2019;62:152966 [eng].
[33] Dong X, Nao J. Relationship between the therapeutic potential of various plant-derived bioactive compounds and their related microRNAs in neurological disorders. Phytomedicine 2023;108:154501 [eng].
[34] Wang L, Yan W, Tian Y, Xue H, Tang J, Zhang L. Self-microemulsifying drug delivery system of phillygenin: formulation development, characterization and pharmacokinetic evaluation. Pharmaceutics 2020;12(2) [eng].
[35] Zhang P, Jin Y, Xia W, Wang X, Zhou Z. Phillygenin inhibits inflammation in chondrocytes via the Nrf2/NF-kappaB axis and ameliorates osteoarthritis in mice. J Orthop Translat 2023;41:1–11.
[36] Wang X, Wang P, Du H, Li N, Jing T, Zhang R, et al. Prediction of the active components and mechanism of forsythia suspensa leaf against respiratory syncytial virus based on network pharmacology. Evid Based Complement Alternat Med 2022;2022:5643345 [eng].
[37] Xiao S, Zhang Y, Liu Z, Li A, Tong W, Xiong X, et al. Alpinetin inhibits neuroinflammation and neuronal apoptosis via targeting the JAK2/STAT3 signaling pathway in spinal cord injury. CNS Neurosci Ther 2023;29(4):1094–108 [eng].
[38] Ahuja CS, Wilson JR, Nori S, Kotter MRN, Druschel C, Curt A, et al. Traumatic spinal cord injury. Nat Rev Dis Prim 2017;3:17018 [eng].
[39] Chio JCT, Punjani N, Hejrati N, Zavvarian MM, Hong J, Fehlings MG. Extracellular matrix and oxidative stress following traumatic spinal cord injury: physiological and pathophysiological roles and opportunities for therapeutic intervention. Antioxidants Redox Signal 2022;37(1–3):184–207 [eng].
[40] Han Q, Xie Y, Ordaz JD, Huh AJ, Huang N, Wu W, et al. Restoring cellular energetics promotes axonal regeneration and functional recovery after spinal cord injury. Cell Metabol 2020;31(3). 623-41.e8. [eng].
[41] Dolci S, Mannino L, Bottani E, Campanelli A, Di Chio M, Zorzin S, et al. Therapeutic induction of energy metabolism reduces neural tissue damage and increases microglia activation in severe spinal cord injury. Pharmacol Res 2022;178:106149 [eng].
[42] Wang Y, Tian M, Tan J, Pei X, Lu C, Xin Y, et al. Irisin ameliorates neuroinflammation and neuronal apoptosis through integrin αVβ5/AMPK signaling pathway after intracerebral hemorrhage in mice. J Neuroinflammation 2022;19(1): 82 [eng].
[43] McNamara NB, Munro DAD, Bestard-Cuche N, Uyeda A, Bogie JFJ, Hoffmann A, et al. Microglia regulate central nervous system myelin growth and integrity. Nature 2023;613(7942):120–9 [eng].
[44] Deczkowska A, Keren-Shaul H, Weiner A, Colonna M, Schwartz M, Amit I. Disease-associated microglia: a universal immune sensor of neurodegeneration. Cell 2018; 173(5):1073–81 [eng].
[45] Kobashi S, Terashima T, Katagi M, Nakae Y, Okano J, Suzuki Y, et al. Transplantation of M2-deviated microglia promotes recovery of motor function after spinal cord injury in mice. Mol Ther 2020;28(1):254–65 [eng].
[46] Rahimifard M, Maqbool F, Moeini-Nodeh S, Niaz K, Abdollahi M, Braidy N, et al. Targeting the TLR4 signaling pathway by polyphenols: a novel therapeutic strategy for neuroinflammation. Ageing Res Rev 2017;36:11–9 [eng].
[47] Zusso M, Lunardi V, Franceschini D, Pagetta A, Lo R, Stifani S, et al. Ciprofloxacin and levofloxacin attenuate microglia inflammatory response via TLR4/NF-kB pathway. J Neuroinflammation 2019;16(1):148.
[48] Wang PF, Xiong XY, Chen J, Wang YC, Duan W, Yang QW. Function and mechanism of toll-like receptors in cerebral ischemic tolerance: from preconditioning to treatment. J Neuroinflammation 2015;12:80 [eng].
[49] Hu L, Si L, Dai X, Dong H, Ma Z, Sun Z, et al. Exosomal miR-409-3p secreted from activated mast cells promotes microglial migration, activation and neuroinflammation by targeting Nr4a2 to activate the NF-κB pathway. J Neuroinflammation 2021;18(1):68 [eng].
[50] Shen Y, Yang R, Zhao J, Chen M, Chen S, Ji B, et al. The histone deacetylase inhibitor belinostat ameliorates experimental autoimmune encephalomyelitis in mice by inhibiting TLR2/MyD88 and HDAC3/NF-κB p65-mediated neuroinflammation. Pharmacol Res 2022;176:105969 [eng].
[51] Ciesielska A, Matyjek M, Kwiatkowska K. TLR4 and CD14 trafficking and its influence on LPS-induced pro-inflammatory signaling. Cell Mol Life Sci 2021;78 (4):1233–61 [eng].
[52] Zhao Z, Ning J, Bao XQ, Shang M, Ma J, Li G, et al. Fecal microbiota transplantation protects rotenone-induced Parkinson's disease mice via suppressing inflammation mediated by the lipopolysaccharide-TLR4 signaling pathway through the microbiota-gut-brain axis. Microbiome 2021;9(1):226 [eng].
[53] Zhao Z, Li F, Ning J, Peng R, Shang J, Liu H, et al. Novel compound FLZ alleviates rotenone-induced PD mouse model by suppressing TLR4/MyD88/NF-κB pathway through microbiota-gut-brain axis. Acta Pharm Sin B 2021;11(9):2859–79 [eng].